INFLAMED FAT: immune modulation of adipose tissue and lipid metabolism

Dam, A.D. van; Dam A.D. van

Chapter 5

Salsalate activates brown adipose tissue in mice

Andrea D. van Dam, Kimberly J. Nahon, Sander Kooijman, Susan M. van den Berg, Anish A. Kanhai, Takuya Kikuchi, Mattijs M. Heemskerk, Vanessa van Harmelen, Marc Lombès, Anita M. van den Hoek, Menno P.J. de Winther, Esther Lutgens, Bruno Guigas, Patrick C.N. Rensen, Mariëtte R. Boon

Diabetes 2015; 64:1544-1554

ABSTRACT

Salsalate improves glucose intolerance and dyslipidemia in type 2 diabetes patients, but the mechanism is still unknown. The aim of the present study was to unravel the molecular mechanisms involved in these beneficial metabolic effects of salsalate by treating mice with salsalate during and after development of high fat diet-induced obesity. We found that salsalate attenuated and reversed high fat diet-induced weight gain, in particular fat mass accumulation, improved glucose tolerance and lowered plasma triglyceride (TG) levels. Mechanistically, salsalate selectively promoted the uptake of fatty acids from glycerol tri[^{3}H]oleate-labeled lipoprotein-like emulsion particles by brown adipose tissue (BAT), decreased the intracellular lipid content in BAT and increased rectal temperature, all pointing to more active BAT. Treatment of differentiated T37i brown adipocytes with salsalate increased uncoupled respiration in cells. Moreover, salsalate upregulated *Ucp1* expression and enhanced glycerol release, a dual effect that was abolished by inhibition of protein kinase A (PKA). In conclusion, salsalate activates BAT, presumably by directly activating brown adipocytes via the PKA pathway, suggesting a novel mechanism that may explain its beneficial metabolic effects in type 2 diabetes patients.

INTRODUCTION

Salsalate is a nonsteroidal anti-inflammatory drug belonging to the salicylate class of drugs. Salicylates are originally derived from plants, in which they function as part of the immune system to combat infections. Nowadays, synthetic compounds that break down to salicylates *in vivo,* including aspirin and salsalate, have largely replaced salicylate (1). In humans, salicylates have strong anti-inflammatory effects and have therefore been applied in the clinic for several decades to treat pain and inflammation caused by rheumatoid arthritis (2, 3).

Studies have shown that salicylates exhibit beneficial metabolic effects as well. A recent trial has demonstrated that salsalate lowers HbA1c levels, fasting blood glucose and circulating triglycerides (TG) in type 2 diabetes patients (4). Furthermore, salsalate increases energy expenditure in human subjects (5). In contrast to aspirin, salsalate is not associated with an increased risk of gastrointestinal bleeding and therefore relatively safe for long-term clinical experience. Thus, it is considered a promising anti-diabetic drug (3). The mechanisms underlying the beneficial metabolic effects of salsalate remain largely unknown, partly because its receptor has not been identified yet (6). Salicylates have been shown to activate AMP-activated protein kinase (AMPK) in liver, muscle and white adipose tissue (WAT), suggesting a role of this energy-sensing kinase in the mechanism of action of the drug (1). However, salicylate still improves glucose metabolism in mice lacking the regulatory AMPK-β1 subunit, suggesting involvement of other pathways as well (1).

The objective of the current study was to investigate the mechanism(s) underlying the beneficial effects of salsalate on lipid and glucose metabolism by treating APOE*3-Leiden.CETP (E3L.CETP) transgenic mice, a well-established model for human-like lipoprotein metabolism (7-9), with salsalate mixed through the high fat diet (HFD). We found that salsalate both prevented and reduced HFD-induced weight gain by lowering fat mass accumulation, and improved glucose and lipid metabolism. Mechanistic studies showed that these effects were accompanied by increased activity of brown adipose tissue (BAT). Taken together, our data indicate that BAT may contribute to the beneficial effects of salsalate on lipid and glucose metabolism and corroborate previous findings that targeting BAT may be a valuable strategy to correct metabolic derangements.

MATERIALS AND METHODS

Mice, diet and salsalate treatment

APOE*3-Leiden cholesteryl ester transfer protein (E3L.CETP) mice were obtained as previously described (7-9). To assess the effect of salsalate on progression of obesity, dyslipidemia and hyperglycemia, 10-week old male E3L.CETP mice were randomized to receive an HFD (Research Diets, 45% kcal lard fat) without or with 0.5% (w/w) salsalate (2-carboxyphenyl salicylate, TCI Europe N.V.) for 12 weeks. To assess the effect of salsalate on regression of obesity and associated metabolic disorders, 10-week old male diet-

induced (12 weeks HFD) obese E3L.CETP mice received salsalate (0.5% w/w) for 4 weeks. To investigate the effect of salsalate independent of the E3L.CETP background in a progression setting, 10-week old male wild-type (WT) mice (C57Bl/6J background; Charles River, USA) were randomized to receive an HFD without or with salsalate for 4 weeks.

Mice were individually housed at 21°C or 28°C (WT mice). To mask the bitter taste of salsalate, anise (3.33%, w/w) was added to the diet of both groups in all studies (10). Mouse experiments were performed in accordance with the Institute for Laboratory Animal Research Guide for the Care and Use of Laboratory Animals and have received approval from the University Ethical Review Board (Leiden University Medical Center, Leiden, The Netherlands).

Body weight and body composition measurements

Body weight was measured with a scale and body composition using EchoMRI (EchoMRI-100, Houston, Texas, USA).

Determination of plasma parameters

Upon randomisation and at 4 week intervals during treatment, 6 h fasted blood was collected and assayed for triglycerides (TG), total cholesterol (TC) and free fatty acids (FFA) as described before (11, 12). Glucose was measured using an enzymatic kits from Instruchemie (Delfzijl) and insulin by ELISA (Crystal Chem. Inc., Downers Grove, IL).

Intravenous Glucose Tolerance Test (ivGTT)

Mice were fasted for 6 h, a baseline blood sample was obtained, and mice were intravenously injected with 10 µl/g body weight of glucose dissolved in PBS (200 mg/mL). Additional blood samples were taken at t = 5, 15, 30, 60, 90 and 120 min. Capillaries were placed on ice and centrifuged, and glucose levels were measured as described above.

In vivo clearance of radiolabeled lipoprotein-like emulsion particles

Lipoprotein-like TG-rich emulsion particles (80 nm) labeled with glycerol tri[^{3}H]oleate (triolein, [^{3}H]TO) were prepared and characterized as described previously (13). Mice were fasted for 6 h (from 7.00 am to 13.00 pm) and injected with 200 µl of emulsion particles (1.0 mg TG per mouse) via the tail vein (t = 0). After 15 min, mice were sacrificed by cervical dislocation and perfused with ice-cold PBS through the heart. Thereafter, organs were harvested, weighed and the uptake of [^{3}H]TO-derived radioactivity was quantified and expressed per gram wet tissue weight.

Rectal temperature measurement

Rectal temperature was measured between 3.00 and 4.00 p.m. using a rectal probe attached to a digital thermometer (BAT-12 Microprobe Thermometer, Physitemp, Clifton, NJ).

Histology

Interscapular BAT and gonadal WAT were removed and fixed in 4% paraformaldehyde, dehydrated in 70% EtOH and embedded in paraffin. Haematoxylin and eosin (H&E) staining was done using standard protocols. The area of intracellular lipid vacuoles in BAT was quantified using Image J (NIH, US).

Quantification of TG content in BAT

Lipids were extracted from BAT following a modified protocol from Bligh and Dyer (14). BAT samples (~50 mg) were homogenized in 10 µL of ice-cold CH_3OH per mg tissue. Lipids were extracted into an organic phase by addition of 1800 µL of CH_3OH:$CHCl_3$ (1:3 v/v) to 45 µL homogenate and subsequent centrifugation. The lower organic phase was evaporated, lipids were resuspended in 2% Triton X-100 and TG content was assayed (see above). BAT lipids were reported per mg protein (Pierce BCA Protein Assay Kit).

Isolation of stromal vascular fraction and flow cytometry

Gonadal WAT was removed, rinsed in PBS and minced. Tissues were digested in a collagenase mixture (DMEM with 20 mM HEPES, Collagenase XI and Collagenase I, Sigma) for 45 min at 37°C and passed through a 70-µm nylon mesh. The suspension was centrifuged (6 min, 1,250 rpm) and the pelleted stromal vascular fraction (SVF) was resuspended in FACS buffer. Fc blocking (CD16/32 antibody) was performed prior to a 30 min staining with fluorescently labeled primary antibodies for CD45, CD11b, Ly6G, F4/80, CD11c, CD206, Gr-1, CD19, CD3, CD4, CD8, CD25 and FoxP3 (BioLegend, e-Bioscience or BD). SVF was analyzed by flow cytometry with a BD FacsCANTO II flow cytometer and FlowJo software.

Analysis of DNA content

DNA content in gonadal WAT samples was quantified as previously described (15).

Culture and differentiation of white and brown adipocytes

3T3-L1 (American Type Culture Collection, Manassas, VA) and T37i cells (16, 17) were cultured and differentiated as described before. Differentiated cells were treated with salsalate (SML0070, Sigma), sodium salicylate (S2007, Sigma), AICA riboside (AICAR; ab120358, Abcam), noradrenalin (A7257, Sigma), CL316243 (Tocris Bioscience, Bristol, UK) or vehicle (DMSO) for 15 min or 8 h. H89 (H-5239, LC Laboratories) was added 1 h before initiation of salsalate treatment. Supernatant was collected for determination of glycerol concentration (Instruchemie, Delfzijl) and cells were harvested for RNA or protein analysis as described below.

Oxygen consumption measurements

A Seahorse Bioscience XF96 extracellular flux analyzer (Seahorse Biosciences, North Billerica, MA) was used to measure oxygen consumption rate (OCR) in differentiated T37i cells. On day 8 of differentiation, cells were trypsinized and seeded in a 96-well Seahorse assay plate. The next day, the ATP synthase inhibitor oligomycin, vehicle, salsalate and

Table 1: *Primary antibodies for Western blot.*

Primary antibody	Residue	Supplier	Reference	Dilution
ACC	-	Cell Signaling	#3662	1:1000
pACC	Ser79	Cell Signaling	#3661	1:1000
AMPKα	-	Cell Signaling	#2532	1:1000
pAMPKα	Thr172	Cell Signaling	#2535	1:1000
pHSL	Ser563	Cell Signaling	#4139	1:1000
pHSL	Ser565	Cell Signaling	#4137	1:1000
PKA substrates	Ser/Thr	Cell Signaling	#9621	1:1000
UCP1	-	Sigma	U6382	1:5000
α/β Tubulin	-	Cell Signaling	#2148	1:1000

Table 2: *Primer sequences of forward and reverse primers (5′ → 3′).*

Gene	Forward primer	Reverse Primer
36b4	GGACCCGAGAAGACCTCCTT	GCACATCACTCAGAATTTCAATGG
Acc1	AACGTGCAATCCGATTTGTT	GAGCAGTTCTGGGAGTTTCG
Acc2	AGATGGCCGATCAGTACGTC	GGGGACCTAGGAAAGCAATC
Adrb3	TGAAACAGCAGACAGGGACA	AGTCTGTCAGCTTCCCTCCA
Cd36	GCAAAGAACAGCAGCAAAATC	CAGTGAAGGCTCAAAGATGG
Cpt1a	AGGAGACAAGAACCCCAACA	AAGGAATGCAGGTCCACATC
Elovl3	TGTTGGCCAGACCTACATGA	ATCCGTGTAGATGGCAAAGC
F4/80	CTTTGGCTATGGGCTTCCAGTC	GCAAGGAGGACAGAGTTTATCGTG
Fasn	CACAGGCATCAATGTCAACC	TTTGGGAAGTCCTCAGCAAC
Fizz1	CCTGCCCTGCTGGGATGACT	GGGCAGTGGTCCAGTCAACGA
Mcp1	GCATCTGCCCTAAGGTCTTCA	TTCACTGTCACACTGGTCACTCCTA
Nos2	TCCTGGACATTACGACCCCT	CTCTGAGGGCTGACACAAGG
Ppargc1α	TGCTAGCGGTTCTCACAGAG	AGTGCTAAGACCGCTGCATT
Pparα	CAACCCGCCTTTTGTCATAC	CCTCTGCCTCTTTGTCTTCG
Scd1	GCTCTACACCTGCCTCTTCGGGAT	TCCAGAGGCGATGAGCCCCG
Srebp1c	CTGGCTGAGGCGGGATGA	TACGGGCCACAAGAAGTAGA
Ucp1	TCAGGATTGGCCTCTACGAC	TGCATTCTGACCTTCACGAC
Ym1	ACAATTAGTACTGGCCCACCAGGAA	TCCTTGAGCCACTGAGCCTTCA
β2m	TGACCGGCTTGTATGCTATC	CAGTGTGAGCCAGGATATA

CL316243 were preloaded in the reagent delivery chambers and pneumatically injected into the wells. Oligomycin was injected to a final concentration of 1.5 µM and the OCR was measured 3 times after mixing. Then, vehicle (0.1% DMSO), salsalate and/or CL316243 were injected and the OCR was measured 6 times in 30 minutes. All OCR measurements were normalized to cell count using Cyquant (Invitrogen).

Western blot analysis

Pieces of snap-frozen mouse tissues (approx. 50 mg) or T37i cells (grown in 3.8 cm^2 wells) were lysed, protein was isolated and Western blots were performed as previously described (11). Primary antibodies and dilutions are listed in **Table 1**. Protein content was corrected for a control mix on each blot and for the housekeeping protein tubulin.

RNA purification and qRT-PCR

RNA was extracted from snap-frozen mouse tissues (approx. 25 mg) or T37i cells (grown in 3.8 cm^2 wells) using Tripure RNA Isolation reagent (Roche). Total RNA (1-2 µg) was reverse transcribed using Moloney Murine Leukemia Virus (M-MLV) Reverse Transcriptase (Sigma) for qRT-PCR to produce cDNA. mRNA expression was normalized to *β2-microglobulin* (*β2m*) and *36b4* mRNA content and expressed as fold change compared to control mice using the ΔΔCT method. The primers sequences used are listed in **Table 2**.

Statistical analysis

All data are expressed as mean ± SEM, unless stated otherwise. Groups were compared with a two-tailed unpaired Student's test and considered statistically significant if $p<0.05$.

RESULTS

Salsalate prevents high fat diet-induced obesity

To investigate the effect of salsalate on the development of obesity, male E3L.CETP mice were fed an HFD with or without salsalate for 12 weeks (*i.e.* progression study). Salsalate prevented the HFD-induced increase in body mass seen in the control group (-80%, 1.6±2.6 vs. 7.9±5.5 g, $p<0.01$; **Fig. 1A**), which was due to a decreased gain in fat mass (-60%, 3.1±2.4 vs. 7.8±4.2, $p<0.05$; **Fig. 1B**) rather than lean mass (**Fig. 1C**). Although salsalate persistently prevented mice from gaining fat mass throughout the treatment period, salsalate decreased food intake only during the first three days (**Fig. 1D**).

Salsalate prevents high fat diet-induced deterioration of glucose and triglyceride metabolism

Next, we assessed whether salsalate protects mice from developing HFD-induced glucose intolerance and dyslipidemia. Although salsalate did not affect fasting glucose levels (**Fig. 2A**), it reduced insulin levels after 4 weeks (-41%, $p<0.05$), 8 weeks (-47%, $p=0.07$) and 12 weeks (-67%, $p<0.05$; **Fig. 2B**) of treatment. In addition, salsalate improved glucose

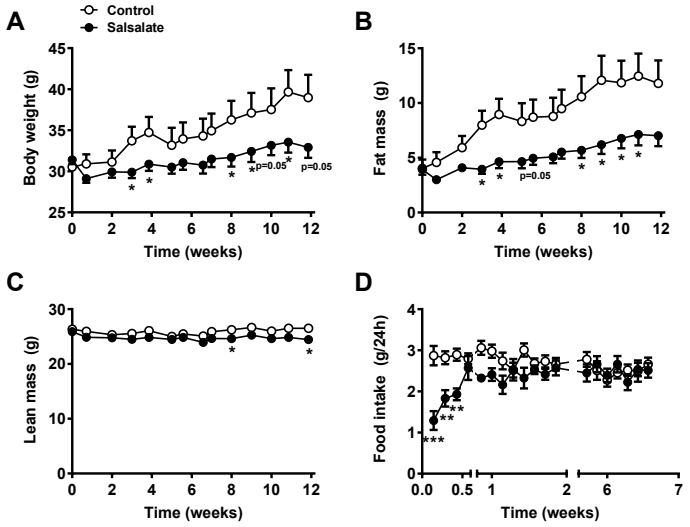

Figure 1. Salsalate prevents obesity and fat mass accumulation in E3L.CETP mice fed a high fat diet. *10-week old male E3L.CETP mice were fed a high fat diet (HFD) without (open circles) or with (closed circles) salsalate for 12 weeks (A-D). Body weight (A), fat mass (B) and lean mass (C) were monitored throughout the experiment. Food intake was measured daily in the first two weeks and in the 6th week of the experiment (D). Values represent means ± SEM (n=9-10). * p<0.05, ** p<0.01, *** p<0.001 vs control.*

tolerance (**Fig. 2C**), as evidenced by a reduction of the area under the curve of glucose concentrations during an ivGTT (AUC -25%, p<0.05; **Fig. 2D**). Salsalate did not affect plasma TC levels **(Fig. 2E)** throughout the treatment period but decreased plasma TG levels at 8 weeks (-43%, p<0.01) and 12 weeks (-47%, p<0.05; **Fig. 2F**).

To elucidate which metabolic organs were involved in the TG-lowering effect of salsalate, the tissue-specific uptake of FA derived from intravenously injected [^{3}H]TO-labeled lipoprotein-like emulsion particles was determined. Salsalate tended to increase the uptake of [^{3}H]TO-derived activity by dorsocervical BAT (dcBAT), although significance was not reached, probably due to the substantial interindividual variation (**Fig. 2G**).

Salsalate reverses high fat diet-induced obesity and improves glucose and triglyceride metabolism

We investigated the potential of salsalate to reverse diet-induced obesity (DIO) in E3L.CETP mice (regression study). In this setting, salsalate lowered body weight (**Fig. 3A**) mainly due to a reduction in fat mass (**Fig. 3B**). Furthermore, salsalate reduced fasting glucose (-30%, p<0.01; **Fig. 3C**) and TG levels (-46%, p<0.05; **Fig. 3D**). Salsalate increased the uptake of [^{3}H]TO-derived activity predominantly by iBAT (+156%, p<0.01) and dcBAT (+102%, p<0.05) and to some extent by the liver (+38%, p<0.01) (**Fig. 3E**). These data suggest that salsalate

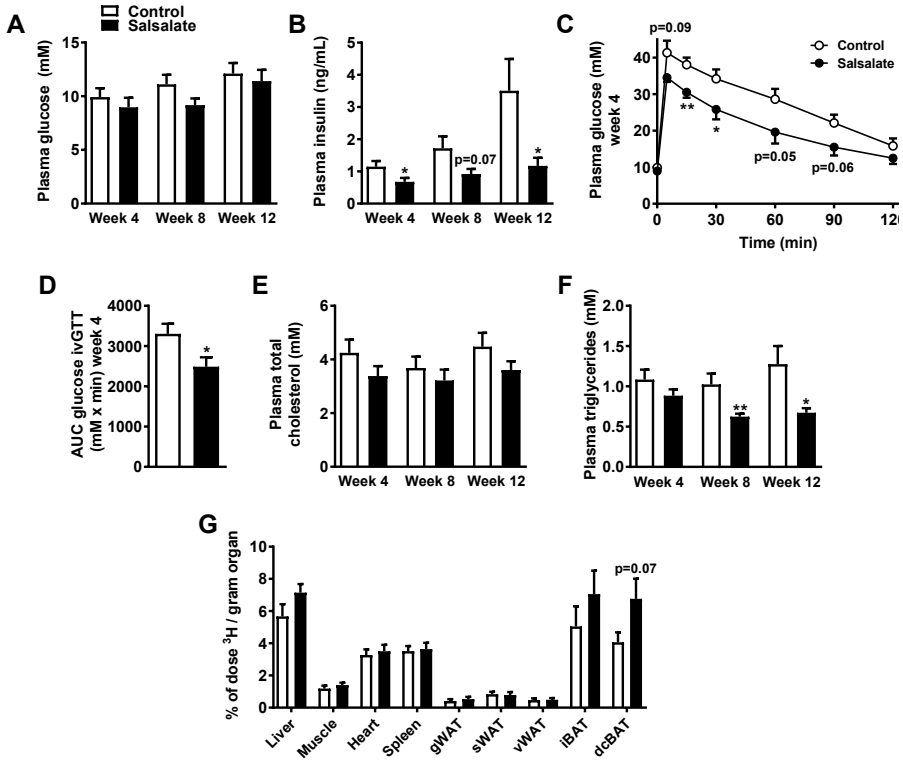

Figure 2. Salsalate prevents high fat diet-induced deterioration of glucose and triglyceride metabolism in E3L.CETP mice fed a high fat diet. *10-week old male E3L.CETP mice were fed a high fat diet (HFD) without (open bars/circles) or with (closed bars/circles) salsalate for 12 weeks (A-G). Blood samples from 6 h-fasted mice were collected by tail vein bleeding at different time points and plasma glucose (A), insulin (B), total cholesterol (E) and triglyceride (F) levels were determined. After 4 weeks, 6 h-fasted mice were injected i.v. with glucose and additional blood samples were taken at 5, 15, 30, 60, 90 and 120 min after injection (C-D). A clearance experiment was performed in which 6 h-fasted mice were i.v. injected with [^{3}H] TO-labeled lipoprotein-like emulsion particles. After 15 min, mice were sacrificed and uptake of [^{3}H]TO-derived activity was determined in the organs (G). AUC = area under the curve. Values represent means ± SEM (n=9-10). * p<0.05, ** p<0.01 vs control. sWAT, subcutaneous white adipose tissue; vWAT, visceral white adipose tissue.*

activates BAT, which is further supported by the observation that rectal temperature was raised (+0.5°C, p<0.05; **Fig. 3F**) upon salsalate treatment. Moreover, salsalate reduced interscapular BAT weight (-50%, p<0.01; **Fig. 3G**), indicating reduced fat accumulation within the tissue. Indeed, lipid droplet content was lower (**Fig. 3H, I, J**), pointing to higher intracellular lipolysis (18).

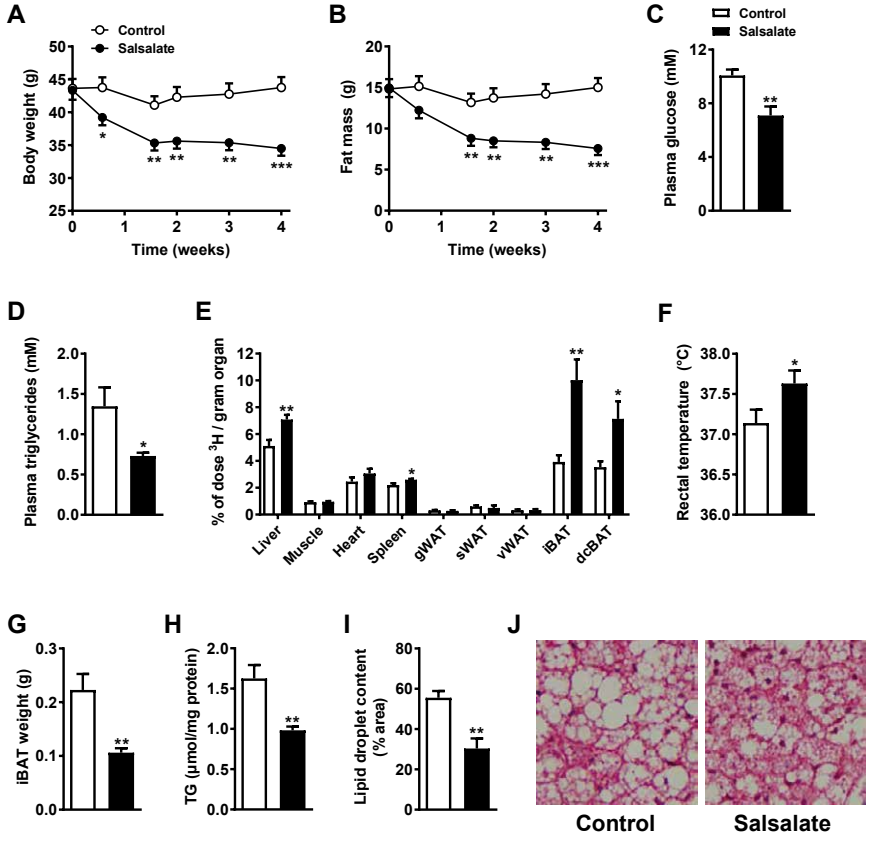

Figure 3. Salsalate reverses high fat diet-induced obesity and deterioration of glucose and triglyceride metabolism and enhances lipoprotein-TG derived fatty acid uptake by liver and brown adipose tissue in E3L.CETP mice fed a high fat diet. *10-week old male E3L.CETP mice were fed an HFD for 12 weeks to render them obese and subsequently fed an HFD without (open bars/circles) or with (closed bars/circles) salsalate for 4 weeks (A-I). Body weight (A) and fat mass (B) were monitored throughout the treatment period. After the treatment period, blood samples from 6 h-fasted mice were collected by tail vein bleeding and plasma glucose (C) and triglyceride (D) levels were determined. A clearance experiment was performed in which 6 h-fasted mice were i.v. injected with [^{3}H]TO-labeled lipoprotein-like emulsion particles. After 15 min, mice were sacrificed and uptake of [^{3}H]TO-derived activity was determined in the organs (E). Rectal temperature was determined after 4 weeks of treatment (F). Upon sacrifice, interscapular brown adipose tissue (iBAT) was collected and weighed (G). Lipids were extracted from BAT and TG content was measured (H). Haematoxylin and Eosin (H&E) staining of BAT sections was performed and relative content of lipid vacuoles in BAT tissue sections were quantified (I), representative pictures are shown (J). Values represent means ± SEM (n=9-10). * p<0.05, ** p<0.01, *** p<0.001 vs control. sWAT, subcutaneous white adipose tissue; vWAT, visceral white adipose tissue.*

Salsalate prevents body weight gain and activates brown adipose tissue irrespective of the transgenic background

To exclude that the effects of salsalate were specific to the E3L.CETP transgenic model, male WT mice were fed an HFD with or without salsalate for 4 weeks. We confirmed that salsalate treatment had similar effects on body weight, body composition and food intake (**Suppl. Fig. 1A-D**). Prevention of adiposity despite equal food intake suggests that either physical activity or energy expenditure is enhanced. Indeed, salsalate increased EE during the dark phase (+10%, $p<0.05$; **Suppl. Fig. 1E**). This was especially due to a higher glucose oxidation (+29%, $p<0.001$; **Suppl. Fig. 1F**), whereas fat oxidation did not differ (**Suppl. Fig. 1G**). Accordingly, respiratory exchange ratio (RER) was higher during the dark phase (**Suppl. Fig. 1H**). Physical activity was not affected (**Suppl. Fig. 1I**), suggesting that the energetic loss is mainly explained by increased energy expenditure.

Comparable to our findings in E3L.CETP mice, salsalate reduced plasma insulin levels (**Suppl. Fig. 2A**) and improved glucose tolerance (**Suppl. Fig. 2B-D**). This was probably achieved via an insulin-independent mechanism, as no differences in glucose levels were found between the treatment groups upon an insulin challenge (**Suppl. Fig. 2E**). Of note, AMPK phosphorylation in muscle was enhanced upon salsalate treatment (+43%, $p<0.05$), as was phosphorylation of its downstream target ACC (+75%, $p<0.05$; **Suppl. Fig. 2**F).

In WT mice, salsalate also reduced plasma triglyceride levels (**Suppl. Fig. 2G**). This was not due to lowered intestinal TG absorption, since salsalate-treated mice did not have significantly lower plasma TG levels in response to an oral olive oil gavage (**Suppl. Fig. 2H**) and FFA content in feces collected in the third week of treatment was unaltered (**Suppl. Fig. 2I**). Neither VLDL-TG (**Suppl. Fig. 2J**) nor VLDL[^{35}S]apoB production (**Suppl. Fig. 2K**) were affected upon 4 weeks of salsalate treatment, further supporting a role for BAT in the TG-lowering effect of salsalate. Indeed, comparable to the effects seen in E3L.CETP mice, salsalate reduced interscapular BAT weight (-42%, $p<0.001$; **Fig. 4A**), lowered lipid content (-29%, $p<0.05$**; Fig. 4B, C**) and tended to increase the uptake of [^{3}H]TO-derived activity by the BAT depots (**Suppl. Fig. 3C**).

Under thermoneutral conditions, salsalate still prevented the development of high fat diet-induced obesity (**Suppl. Fig. 3A,B**). However, thermoneutrality ablated the salsalate-induced tendency towards an increased TG uptake by BAT (**Suppl. Fig. 3C**) and prevented the reduction in plasma TG levels seen at room temperature (**Suppl. Fig. 3D**). Thus, noradrenergic input (*i.e.* slight cold sensing at room temperature) seems necessary to bring about salsalate-induced TG uptake by BAT.

To further elucidate the mechanisms by which salsalate activates BAT and regulates intracellular lipolysis, we measured mRNA and (phosphorylated) protein levels in BAT of mice housed at 21°C upon treatment. Salsalate did not affect *Ucp1* mRNA expression (data not shown) nor UCP1 protein content (**Fig. 4D**). Salsalate tended to increase the PKA-mediated lipolysis-stimulating phosphorylation of HSL on the Ser563 residue (+77%, $p=0.06$) but not AMPK-mediated phosphorylation of HSL on the Ser565 residue (19) (**Fig. 4D**), suggesting increased PKA signaling in BAT. Despite the fact that phosphorylation of ACC, the downstream target of AMPK, was increased, we did not observe significant differences in AMPK expression or phosphorylation (**Fig. 4D**).

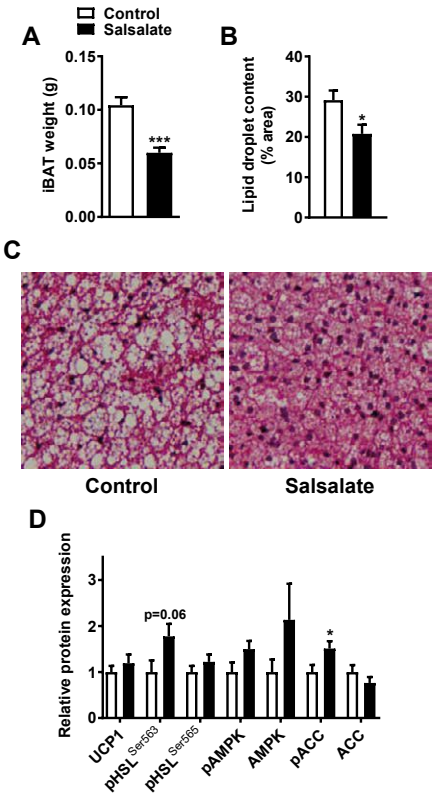

Figure 4. Salsalate activates brown adipose tissue in wild type mice fed a high fat diet. *10-week old male C57Bl/6J mice were fed a high fat diet (HFD) without (open bars) or with (closed bars) salsalate for 4 weeks. Upon sacrifice, interscapular brown adipose tissue (iBAT) was collected and weighed (A). Haematoxylin and Eosin (H&E) staining of BAT sections was performed and relative content of lipid vacuoles in BAT tissue sections were quantified (B), representative pictures are shown (C). Protein content was determined by Western blot (D). Values represent means ± SEM (n=6-8). * p<0.05, *** p<0.001 vs control.*

Salsalate reduces WAT cell size and lowers inflammation in wild type mice fed a high fat diet

Since salsalate massively reduced fat mass, we assessed the phenotype of WAT in more detail. In line with the decreased total fat mass (**Figs. 1B, 3B, S1B**), salsalate reduced the weight of the gonadal WAT (gWAT) fat pad (-49%, p<0.001; **Fig. 5A**). Histological analysis showed that salsalate reduced adipocyte size (-44%, p<0.01; **Figs. 5B, C**), while total cell number, as assessed by DNA content, did not differ (data not shown).

Since salsalate is an anti-inflammatory compound, we investigated the immune cell composition of gWAT by flow cytometry. We did not observe a change in the percentage of CD45+ cells within the stromal vascular fraction (SVF), nor in relative monocyte, macrophage, granulocyte, T- and B-cell content (data not shown). However, we found less pro-inflammatory (CD11c+) M1 macrophages and more anti-inflammatory (CD206+) M2 macrophages within the F4/80+ fraction (**Fig. 5D, E**). Accordingly, salsalate decreased *F4/80* and *Mcp1* mRNA expression in gWAT (**Fig. 5F**), confirming fewer pro-inflammatory macrophages and less recruitment of pro-inflammatory macrophages (20, 21) in gWAT

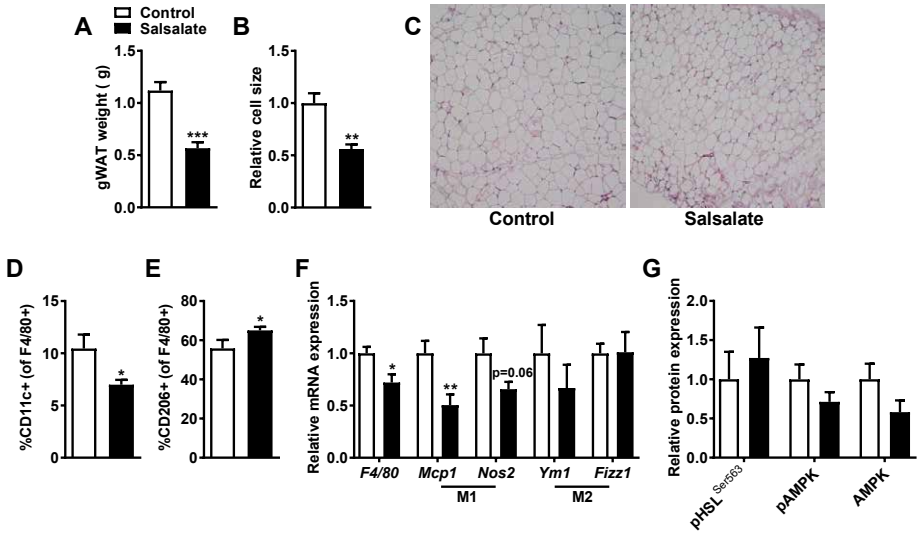

Figure 5. Salsalate reduces white adipocyte cell size and lowers inflammation in WAT of wild type mice fed a high fat diet. *10-week old male wild type mice were fed a high fat diet (HFD) without (open bars) or with (closed bars) salsalate for 4 weeks. Gonadal white adipose tissue (gWAT) was collected and weighed (A). Haematoxylin and Eosin (H&E) staining of gWAT sections was performed and relative cell size of white adipocytes in gWAT tissue sections was quantified (B), representative pictures are shown (C). Percentage of macrophages (%CD11b$^+$Ly6G$^-$F4/80$^+$) of CD45$^+$ cells in stromal vascular fraction (SVF) of gWAT were determined by flow cytometry. Within the macrophage fraction, pro-inflammatory M1 macrophages (CD11c$^+$) (D) and anti-inflammatory M2 macrophages (CD206$^+$) (E) were measured. mRNA expression in of inflammatory markers (F) in gWAT was determined by qRT-PCR. Protein content was determined by Western blot (G). Values represent means ± SEM (n=6-8). * p<0.05, ** p<0.01, *** p<0.001 vs control.*

of salsalate treated mice. Thus, besides preventing fat accumulation in WAT, salsalate prevented HFD-induced skewing of macrophages towards a pro-inflammatory phenotype.

Next, we studied whether the diminished adipocyte size following salsalate treatment could be the result of increased TG lipolysis. Phosphorylation levels of HSL on the Ser563 residue (phosphorylated by PKA; **Fig. 5G**) in gWAT did not differ, nor did plasma free fatty acid (FFA) levels (data not shown). Moreover, *in vitro* stimulation of 3T3-L1 cells with salsalate did not influence Ser563-HSL phosphorylation (**Suppl. Fig. 4A**) and even repressed the glycerol concentration in the supernatant (**Suppl. Fig. 4B**). Of the oxidation genes we measured in gWAT, only *Acc2* was upregulated upon salsalate treatment, suggesting slightly enhanced oxidation in gWAT (**Suppl. Fig. 5A**). The phosphorylation state nor the expression of AMPK was altered (**Fig. 5G**) in gWAT. We also investigated markers of lipogenesis in gWAT, but only found an upregulation of *Acc1* expression (**Suppl. Fig. 5B**). Collectively, these data indicate that it is unlikely that lipolysis, oxidation or lipogenesis in WAT is the primary mechanism responsible for the prevention of fat mass accumulation following salsalate treatment.

Salsalate directly activates brown adipocytes in vitro

Since our collective data suggested that the improvement in triglyceride metabolism by salsalate could be due to activation of BAT, we investigated whether salsalate directly activates brown adipocytes and which intracellular mechanism(s) are involved. Strikingly, treatment of differentiated T37i adipocytes with salsalate increased uncoupled respiration (**Fig. 6A**). In line with this, increasing concentrations of salsalate resulted in a dose-dependent increase in *Ucp1* expression (up to +227%, p<0.001; **Fig. 6B**) as well as glycerol release (up to +92%, p<0.001; **Fig. 6C**). Accordingly, salsalate decreased lipid content in the cells, as shown by Nile Red staining (-18%, p<0.05; **Suppl. Fig. 6A**). Decreased *de novo* lipogenesis found upon treatment with salsalate (**Suppl. Fig. 6B**) could also contribute to this finding. Besides *Ucp1*, salsalate upregulated several other genes involved in BAT function (**Fig. 6D**).

The majority, but not all, of orally administered salsalate is metabolized to salicylate *in vivo*, resulting in plasma concentrations of 1-3 mM (1). Like salsalate, salicylate (1 mM) enhanced *Ucp1* expression in T37i brown adipocytes (+53%, p<0.01, **Suppl. Fig. 6C**). Salicylate (1 and 3 mM) also enhanced expression of *Pparα* (up to +304%, p<0.01) and its target gene (22) *Elovl3* (up to +224%, p<0.05; **Suppl. Fig. 6C**), while the higher dosage of salicylate (3 mM) enhanced glycerol release (+80%, p<0.01; **Suppl. Fig. 6D**).

Since salsalate is known to directly activate AMPK (1), we investigated this in brown adipocytes. However, salsalate did not increase phosphorylation of AMPK (**Fig. 6E**) nor ACC (data not shown) after stimulation for 15 min, 1 h or 8 h (data not shown). We therefore searched for another route by which salsalate may activate BAT.

As both AMPK and PKA regulate lipolysis in BAT by phosphorylation of HSL (23, 24), and our *in vivo* data indicated PKA-mediated phosphorylation of HSL on the Ser563 residue, we investigated whether salsalate activates the PKA-HSL route in brown adipocytes. Salsalate enhanced phosphorylation of the 30 kDa PKA substrate in brown adipocytes

Figure 6 (right page). Salsalate directly activates T37i brown adipocytes. *T37i cells were cultured and differentiated into mature brown adipocytes. Cells were treated with salsalate (300 μM) after addition of oligomycin and oxygen consumption rate was directly measured with an extracellular flux analyzer. Values represent means ± SEM of 11-13 independent wells (A). Cells were treated with increasing concentrations of salsalate for 8 h and Ucp1 mRNA expression (B) and glycerol release (C) were determined. Cells were treated with salsalate (300 μM) for 8 h and mRNA expression was determined (D). Cells were treated with salsalate (300 μM) or AICAR for 15 min and protein content was determined (E). Cells were treated with salsalate (300 μM) for 8 h and protein content was determined (F). Cells were treated with salsalate (300 μM) in the presence of H89 for 8 h and Ser563-HSL phosphorylation (G), Ucp1 mRNA expression (H) and glycerol release (I) were determined. Cells were treated with salsalate (300 μM) and CL316243 (10μM) after addition of oligomycin and oxygen consumption rate was directly measured with an extracellular flux analyzer. Values represent means ± SEM of 11-13 independent wells (J). Protein content was determined by Western Blot and mRNA expression was determined by qRT-PCR. OCR = oxygen consumption rate, OM = oligomycin. Values represent means ± SD of 3-6 independent sets of RNA, supernatant or protein. * p<0.05, ** p<0.01, *** p<0.001 vs control or CL316243, # p<0.05, ## p<0.01 vs salsalate.*

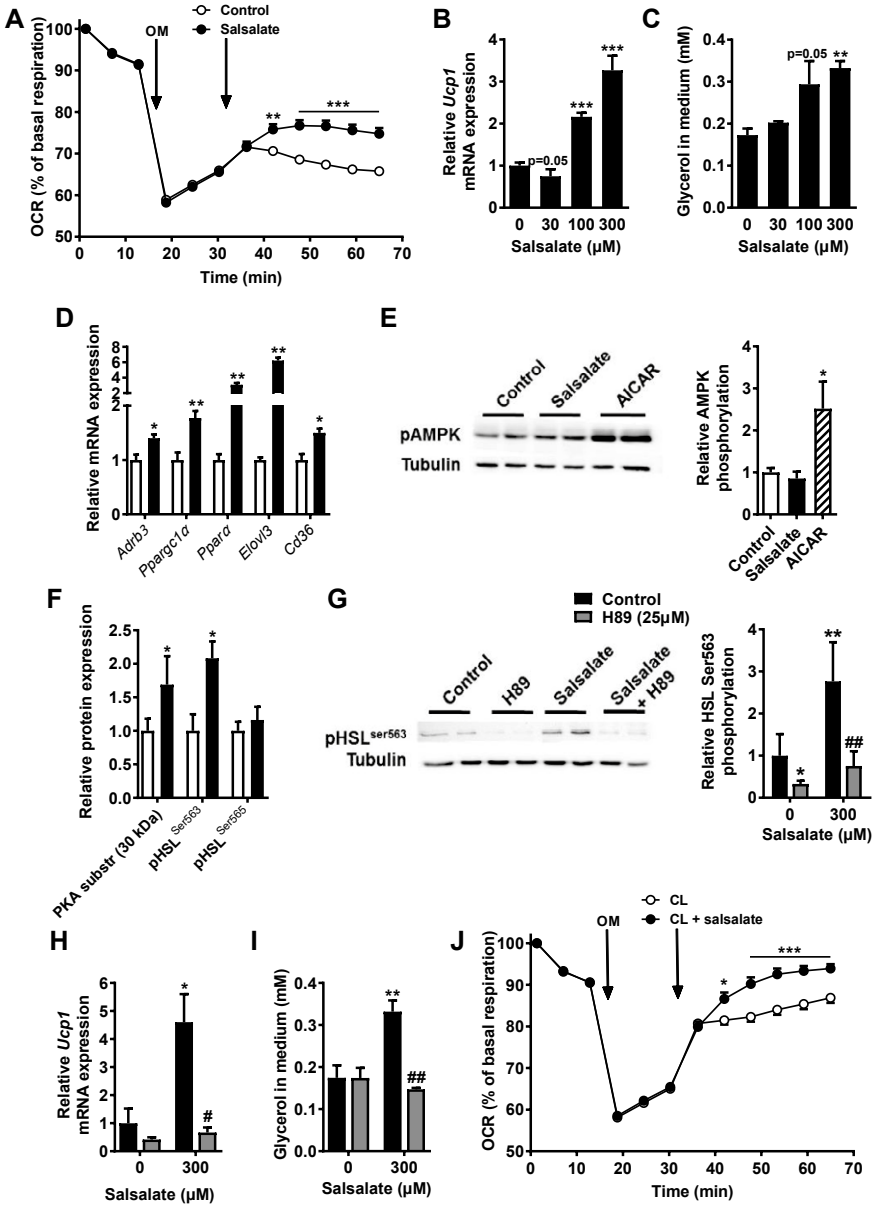
A
Control
Salsalate
OM
OCR (% of basal respiration)
Time (min)
B
Relative Ucp1 mRNA expression
p=0.05
Salsalate (μM)
C
Glycerol in medium (mM)
p=0.05
Salsalate (μM)
D
Relative mRNA expression
Adrb3
Ppargc1α
Pparα
Elovl3
Cd36
E
Control
Salsalate
AICAR
pAMPK
Tubulin
Relative AMPK phosphorylation
F
Relative protein expression
PKA substr (30 kDa)
pHSL Ser563
pHSL Ser565
G
Control
H89 (25μM)
Control
H89
Salsalate
Salsalate + H89
pHSL ser563
Tubulin
Relative HSL Ser563 phosphorylation
Salsalate (μM)
H
Relative Ucp1 mRNA expression
Salsalate (μM)
I
Glycerol in medium (mM)
Salsalate (μM)
J
CL
CL + salsalate
OM
OCR (% of basal respiration)
Time (min)

after 8 h of stimulation (+69%, $p<0.05$) and increased phosphorylation of HSL on Ser563, the PKA phosphorylation site of this lipolytic enzyme (+108%, $p<0.05$; **Fig. 6F**), while phosphorylation of HSL on Ser565, the AMPK phosphorylation site, was unaffected. To investigate the involvement of the PKA pathway for BAT activation by salsalate, we stimulated brown adipocytes with salsalate in the presence of the PKA inhibitor H89 (25 μM). H89 blunted the salsalate-induced Ser563-HSL phosphorylation (**Fig. 6G**), upregulation of *Ucp1* expression (**Fig. 6H**) and glycerol release (**Fig. 6I**), indicating that the PKA pathway is required for brown adipocyte activation by salsalate. These data are consistent with our observation that salsalate only increased TG uptake by BAT *in vivo* when mice are housed at room temperature, *i.e.* when adrenergic signalling is present.

Since PKA is a downstream target of β-adrenergic signalling, we investigated whether salsalate acts in synergism with β-adrenergic stimulation in T37i brown adipocytes. Although salsalate in combination with the β3-agonist CL316243 enhanced uncoupled respiration as compared to CL316243 alone, no synergistic effect was found (**Fig. 6J**). Furthermore, salsalate and NA showed an additive effect on *Ucp1* expression (**Suppl. Fig. 6E**). This suggests that increased β-adrenergic signalling is not required for the effects of salsalate, but since inhibition of PKA abolishes the effects of salsalate, basal β-adrenergic signalling is. Taken together, both our *in vitro* and *in vivo* data point to an interplay between β-adrenergic and salsalate-induced signalling.

DISCUSSION

Previous studies in humans and animals have shown that salsalate has beneficial metabolic effects by improving glucose tolerance and lowering plasma triglycerides (3, 4). The mechanisms responsible for these changes, however, remained unclear. In the present study, we show that chronic treatment of E3L.CETP and WT mice with salsalate recapitulates these beneficial metabolic effects and in addition prevents and reduces body weight gain, mainly by lowering fat mass accumulation. Moreover, we provide evidence from both *in vivo* and *in vitro* studies that salsalate activates BAT, an important player in energy metabolism. To the best of our knowledge, this is the first study reporting that activation of BAT may, at least partly, underlie the beneficial metabolic effects of salsalate.

The finding that salsalate prevented body weight gain and fat mass accumulation accompanied by a reduced white adipocyte size has been reported before in rats (25). Lower fat accumulation may be the consequence of a lower food intake or higher energy expenditure. Although we noticed that food intake was transiently reduced upon salsalate treatment in mice, the preventive effect on fat mass accumulation persisted throughout the studies. We found increased energy expenditure in our study, which is in line with studies in humans showing that salsalate treatment increases energy expenditure by +18% (2, 5), suggesting that the long term inhibiting effects of salsalate on body weight gain are caused by increased resting energy expenditure.

In our study, salsalate improved glucose tolerance via an insulin-independent mechanism and lowered plasma glucose and triglyceride levels, which is in line with findings in humans (2, 3). Recently, it has been shown that salicylate acutely stimulates phosphorylation of AMPK and simultaneously increases glucose transport, independent of insulin, into muscle in rat skeletal muscles *ex vivo* (26). Correspondingly, in our study, AMPK phosphorylation in muscle was enhanced upon salsalate treatment, as was phosphorylation of its downstream target ACC. Taken together, our data suggest that salsalate improves glucose tolerance by enhancing glucose oxidation and glucose uptake via an insulin-independent pathway. BAT, a metabolically active tissue that contributes to energy metabolism by uncoupling the electron transport chain from ATP synthesis through uncoupling protein-1 (UCP1), also has a key role in systemic glucose homeostasis by enhancing glucose clearance (27, 28). Although we do not have evidence for the possibility that salsalate improves glucose tolerance through BAT activation, we did show that the TG-lowering effect of salsalate was due to higher uptake of lipoprotein-TG-derived FA by BAT as intestinal TG absorption and hepatic VLDL production were unaffected in our experimental settings. We provide strong evidence that BAT was activated upon salsalate treatment, since we found reduced intracellular lipid content and higher rectal temperature *in vivo*, and higher uncoupled respiration, upregulation of the expression of thermogenic markers *Ucp1* and *Elovl3* and increased glycerol release upon salsalate treatment *in vitro.*

Regarding the mechanism through which salsalate activates BAT, we found slightly increased phosphorylation of AMPK's downstream target ACC in BAT *in vivo*, but not of AMPK itself. In T37i brown adipocytes *in vitro*, phosphorylation statuses of AMPK and ACC

were also unaffected. Although a recent study by Hawley *et al.* (1) showed that salicylate activates AMPK in the liver, muscle and adipose tissue, they also observed that the potency of salicylate to improve fasting glucose and insulin, glucose tolerance and insulin resistance were retained in mice lacking the β1 subunit of AMPK, demonstrating that other pathways are more important than the AMPK-mediated beneficial metabolic effects of salicylates.

Our data point more profoundly towards activation of the PKA-HSL pathway in BAT. We found that salsalate increased Ser563-HSL phosphorylation in BAT *in vivo* and in brown adipocytes *in vitro*, which points to an increase of PKA-mediated lipolysis. Indeed, salsalate treatment enhanced glycerol release *in vitro* and reduced the intracellular lipid content in BAT *in vivo*. The enhanced intracellular release of FA results in increased availability of substrate for oxidation that can also induce allosteric activation of UCP1 (29), both resulting in enhanced uncoupling, which we also demonstrated in brown adipocytes *in vitro*. Importantly, the fact that PKA inhibition blunted the salsalate-induced Ser563-HSL phosphorylation, *Ucp1* expression and glycerol release *in vitro* supports a necessity for this pathway in brown adipocyte activation.

Besides improving metabolism, salsalate is an effective anti-inflammatory agent in the clinic. With the current knowledge of a profound link between obesity, inflammation and type 2 diabetes, we also investigated the effects of salsalate on the inflammatory state of WAT. In gWAT, salsalate lowered *Mcp1* expression, an attraction factor of pro-inflammatory M1 macrophages, and prevented HFD-induced skewing of macrophages towards this phenotype. Previous research showed that high concentrations of salicylates inhibit NF-κB activity *in vitro*, a key transcription factor that regulates inflammation (30). In obese humans, salsalate lowers the inflammatory state, with a 34% reduction in circulating levels of C-reactive protein and declined NF-κB activity in WAT (31, 32). This reduction in inflammation might contribute to the improved glucose metabolism upon salsalate.

Since it is becoming increasingly clear that BAT activation and subsequent elevation of energy expenditure can lower body fat mass in human adults (33), drugs that target BAT are of great interest in the combat against obesity. Although some human studies suggested that salsalate does not affect body weight (4, 34), effects on fat mass have not been reported. As mice have a relatively larger amount of BAT compared to humans (35, 36), activation of BAT by salsalate in humans might translate into improved fat distribution, glucose and lipid metabolism without substantially affecting total body weight.

In conclusion, we show that salsalate exerts beneficial metabolic effects by directly activating BAT through modulation of the PKA pathway in BAT (**Fig. 7**). Further studies are warranted to investigate whether salsalate activates BAT in humans, thereby preventing obesity and associated disorders.

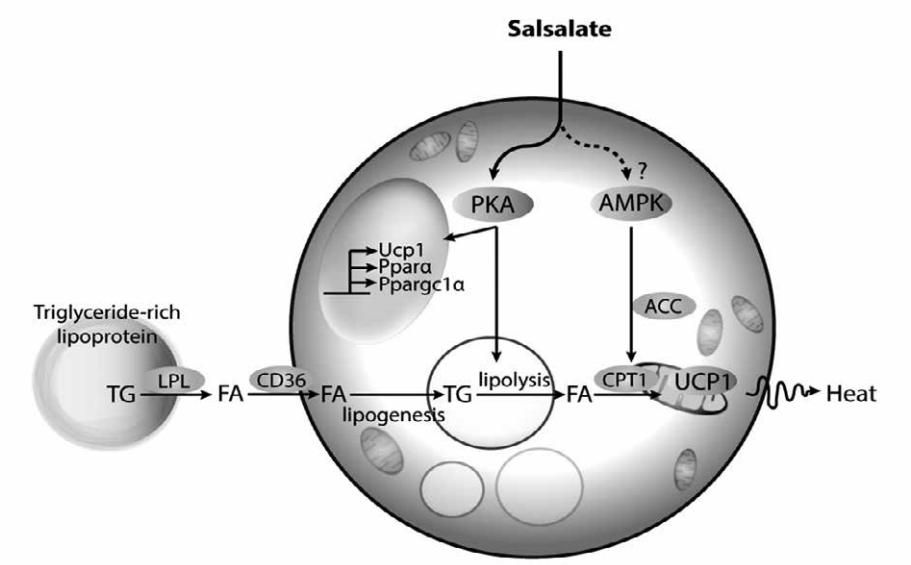

Figure 7. Proposed mechanism by which salsalate activates brown adipose tissue. *Salsalate improves intracellular lipolytic capacity of the brown adipocyte by increasing PKA-mediated HSL phosphorylation, thereby enhancing FA release from TG stored in lipid droplets. This leads to activation of UCP1, which uncouples ATP synthesis. Moreover, salsalate results in enhanced expression of Pparα, Ppargc1α, and Ucp1, altogether resulting in increased activity and uncoupling of ATP synthesis in BAT. A reduction in intracellular lipid content and upregulation of Cd36 in BAT enhances uptake of TG-derived FA from the plasma by BAT. This eventually results in lowering of circulating lipids and reduction in fat mass.*

ACKNOWLEDGEMENTS

The authors are grateful to Annika Tanke, Ellemiek de Wit, Isabel Mol, Hetty Sips, Trea Streefland and Chris van der Bent (all from Leiden University Medical Center, The Netherlands) for their valuable technical assistance.

FUNDING

This work was supported by a research grant of the Rembrandt Institute of Cardiovascular Science (RICS) to PCN Rensen, E Lutgens and MPJ de Winther, and by a personal grant of the Board of Directors of LUMC to MR Boon. PCN Rensen is an Established Investigator of the Dutch Heart Foundation (2009T038).

REFERENCES

1. Hawley SA, Fullerton MD, Ross FA, Schertzer JD, Chevtzoff C, Walker KJ, Peggie MW, Zibrova D, Green KA, Mustard KJ, Kemp BE, Sakamoto K, Steinberg GR, Hardie DG: The ancient drug salicylate directly activates AMP-activated protein kinase. Science (New York, NY) 2012;336:918-922
2. Goldfine AB, Silver R, Aldhahi W, Cai D, Tatro E, Lee J, Shoelson SE: Use of salsalate to target inflammation in the treatment of insulin resistance and type 2 diabetes. Clinical and translational science 2008;1:36-43
3. Rumore MM, Kim KS: Potential role of salicylates in type 2 diabetes. The Annals of pharmacotherapy 2010;44:1207-1221
4. Goldfine AB, Fonseca V, Jablonski KA, Pyle L, Staten MA, Shoelson SE: The effects of salsalate on glycemic control in patients with type 2 diabetes: a randomized trial. Annals of internal medicine 2010;152:346-357
5. Meex RC, Phielix E, Moonen-Kornips E, Schrauwen P, Hesselink MK: Stimulation of human whole-body energy expenditure by salsalate is fueled by higher lipid oxidation under fasting conditions and by higher oxidative glucose disposal under insulin-stimulated conditions. The Journal of clinical endocrinology and metabolism 2011;96:1415-1423
6. Fu ZQ, Yan S, Saleh A, Wang W, Ruble J, Oka N, Mohan R, Spoel SH, Tada Y, Zheng N, Dong X: NPR3 and NPR4 are receptors for the immune signal salicylic acid in plants. Nature 2012;486:228-232
7. de Haan W, van der Hoogt CC, Westerterp M, Hoekstra M, Dallinga-Thie GM, Princen HM, Romijn JA, Jukema JW, Havekes LM, Rensen PC: Atorvastatin increases HDL cholesterol by reducing CETP expression in cholesterol-fed APOE*3-Leiden.CETP mice. Atherosclerosis 2008;197:57-63
8. van der Hoogt CC, de Haan W, Westerterp M, Hoekstra M, Dallinga-Thie GM, Romijn JA, Princen HM, Jukema JW, Havekes LM, Rensen PC: Fenofibrate increases HDL-cholesterol by reducing cholesteryl ester transfer protein expression. Journal of lipid research 2007;48:1763-1771
9. Westerterp M, van der Hoogt CC, de Haan W, Offerman EH, Dallinga-Thie GM, Jukema JW, Havekes LM, Rensen PC: Cholesteryl ester transfer protein decreases high-density lipoprotein and severely aggravates atherosclerosis in APOE*3-Leiden mice. Arteriosclerosis, thrombosis, and vascular biology 2006;26:2552-2559
10. Coomans CP, Geerling JJ, van den Berg SA, van Diepen HC, Garcia-Tardon N, Thomas A, Schroder-van der Elst JP, Ouwens DM, Pijl H, Rensen PC, Havekes LM, Guigas B, Romijn JA: The insulin sensitizing effect of topiramate involves KATP channel activation in the central nervous system. British journal of pharmacology 2013;170:908-918
11. Boon MR, Kooijman S, van Dam AD, Pelgrom LR, Berbée JF, Visseren CA, van Aggele RC, van den Hoek AM, Sips HC, Lombes M, Havekes LM, Tamsma JT, Guigas B, Meijer OC, Jukema JW, Rensen PC: Peripheral cannabinoid 1 receptor blockade activates brown adipose tissue and diminishes dyslipidemia and obesity. FASEB journal : official publication of the Federation of American Societies for Experimental Biology 2014;28:5361-5375
12. Zambon A, Hashimoto SI, Brunzell JD: Analysis of techniques to obtain plasma for measurement of levels of free fatty acids. Journal of lipid research 1993;34:1021-1028
13. Rensen PC, van Dijk MC, Havenaar EC, Bijsterbosch MK, Kruijt JK, van Berkel TJ: Selective liver targeting of antivirals by

recombinant chylomicrons--a new therapeutic approach to hepatitis B. Nature medicine 1995;1:221-225

14. Bligh EG, Dyer WJ: A rapid method of total lipid extraction and purification. Canadian journal of biochemistry and physiology 1959;37:911-917
15. Cariou B, Postic C, Boudou P, Burcelin R, Kahn CR, Girard J, Burnol AF, Mauvais-Jarvis F: Cellular and molecular mechanisms of adipose tissue plasticity in muscle insulin receptor knockout mice. Endocrinology 2004;145:1926-1932
16. Zennaro MC, Le Menuet D, Viengchareun S, Walker F, Ricquier D, Lombes M: Hibernoma development in transgenic mice identifies brown adipose tissue as a novel target of aldosterone action. The Journal of clinical investigation 1998;101:1254-1260
17. van den Berghe N, Ouwens DM, Maassen JA, van Mackelenbergh MG, Sips HC, Krans HM: Activation of the Ras/mitogen-activated protein kinase signaling pathway alone is not sufficient to induce glucose uptake in 3T3-L1 adipocytes. Molecular and cellular biology 1994;14:2372-2377
18. Ortega-Molina A, Efeyan A, Lopez-Guadamillas E, Munoz-Martin M, Gomez-Lopez G, Canamero M, Mulero F, Pastor J, Martinez S, Romanos E, Mar Gonzalez-Barroso M, Rial E, Valverde AM, Bischoff JR, Serrano M: Pten positively regulates brown adipose function, energy expenditure, and longevity. Cell metabolism 2012;15:382-394
19. Watt MJ, Holmes AG, Pinnamaneni SK, Garnham AP, Steinberg GR, Kemp BE, Febbraio MA: Regulation of HSL serine phosphorylation in skeletal muscle and adipose tissue. American journal of physiology Endocrinology and metabolism 2006;290:E500-508
20. Kanda H, Tateya S, Tamori Y, Kotani K, Hiasa K, Kitazawa R, Kitazawa S, Miyachi H, Maeda S, Egashira K, Kasuga M: MCP-1 contributes to macrophage infiltration into adipose tissue, insulin resistance, and hepatic steatosis in obesity. The Journal of clinical investigation 2006;116:1494-1505
21. Weisberg SP, McCann D, Desai M, Rosenbaum M, Leibel RL, Ferrante AW, Jr.: Obesity is associated with macrophage accumulation in adipose tissue. The Journal of clinical investigation 2003;112:1796-1808
22. Jakobsson A, Jorgensen JA, Jacobsson A: Differential regulation of fatty acid elongation enzymes in brown adipocytes implies a unique role for Elovl3 during increased fatty acid oxidation. American journal of physiology Endocrinology and metabolism 2005;289:E517-526
23. Geerling JJ, Boon MR, van der Zon GC, van den Berg SA, van den Hoek AM, Lombes M, Princen HM, Havekes LM, Rensen PC, Guigas B: Metformin lowers plasma triglycerides by promoting VLDL-triglyceride clearance by brown adipose tissue in mice. Diabetes 2014;63:880-891
24. Cannon B, Nedergaard J: Brown adipose tissue: function and physiological significance. Physiological reviews 2004;84:277-359
25. Cao Y, Dubois DC, Sun H, Almon RR, Jusko WJ: Modeling diabetes disease progression and salsalate intervention in Goto-Kakizaki rats. The Journal of pharmacology and experimental therapeutics 2011;339:896-904
26. Serizawa Y, Oshima R, Yoshida M, Sakon I, Kitani K, Goto A, Tsuda S, Hayashi T: Salicylate acutely stimulates 5'-AMP-activated protein kinase and insulin-independent glucose transport in rat skeletal muscles. Biochemical and biophysical research communications 2014;453:81-85
27. Stanford KI, Middelbeek RJ, Townsend KL, An D, Nygaard EB, Hitchcox KM, Markan KR, Nakano K, Hirshman MF, Tseng YH, Goodyear LJ: Brown adipose tissue regulates glucose homeostasis and insulin sensitivity. The Journal of clinical investigation 2013;123:215-223

28. Matsushita M, Yoneshiro T, Aita S, Kameya T, Sugie H, Saito M: Impact of brown adipose tissue on body fatness and glucose metabolism in healthy humans. International journal of obesity (2005) 2014;38:812-817
29. Fedorenko A, Lishko PV, Kirichok Y: Mechanism of fatty-acid-dependent UCP1 uncoupling in brown fat mitochondria. Cell 2012;151:400-413
30. Kopp E, Ghosh S: Inhibition of NF-kappa B by sodium salicylate and aspirin. Science (New York, NY) 1994;265:956-959
31. Goldfine AB, Fonseca V, Jablonski KA, Chen YD, Tipton L, Staten MA, Shoelson SE: Salicylate (salsalate) in patients with type 2 diabetes: a randomized trial. Annals of internal medicine 2013;159:1-12
32. Fleischman A, Shoelson SE, Bernier R, Goldfine AB: Salsalate improves glycemia and inflammatory parameters in obese young adults. Diabetes care 2008;31:289-294
33. Yoneshiro T, Aita S, Matsushita M, Kayahara T, Kameya T, Kawai Y, Iwanaga T, Saito M: Recruited brown adipose tissue as an antiobesity agent in humans. The Journal of clinical investigation 2013;123:3404-3408
34. Koska J, Ortega E, Bunt JC, Gasser A, Impson J, Hanson RL, Forbes J, de Courten B, Krakoff J: The effect of salsalate on insulin action and glucose tolerance in obese non-diabetic patients: results of a randomised double-blind placebo-controlled study. Diabetologia 2009;52:385-393
35. van Marken Lichtenbelt WD, Schrauwen P: Implications of nonshivering thermogenesis for energy balance regulation in humans. American journal of physiology Regulatory, integrative and comparative physiology 2011;301:R285-296
36. Vosselman MJ, van Marken Lichtenbelt WD, Schrauwen P: Energy dissipation in brown adipose tissue: from mice to men. Molecular and cellular endocrinology 2013;379:43-50
37. Van Klinken JB, van den Berg SA, Havekes LM, Willems Van Dijk K: Estimation of activity related energy expenditure and resting metabolic rate in freely moving mice from indirect calorimetry data. PloS one 2012;7:e36162
38. Redgrave TG, Roberts DC, West CE: Separation of plasma lipoproteins by density-gradient ultracentrifugation. Analytical biochemistry 1975;65:42-49

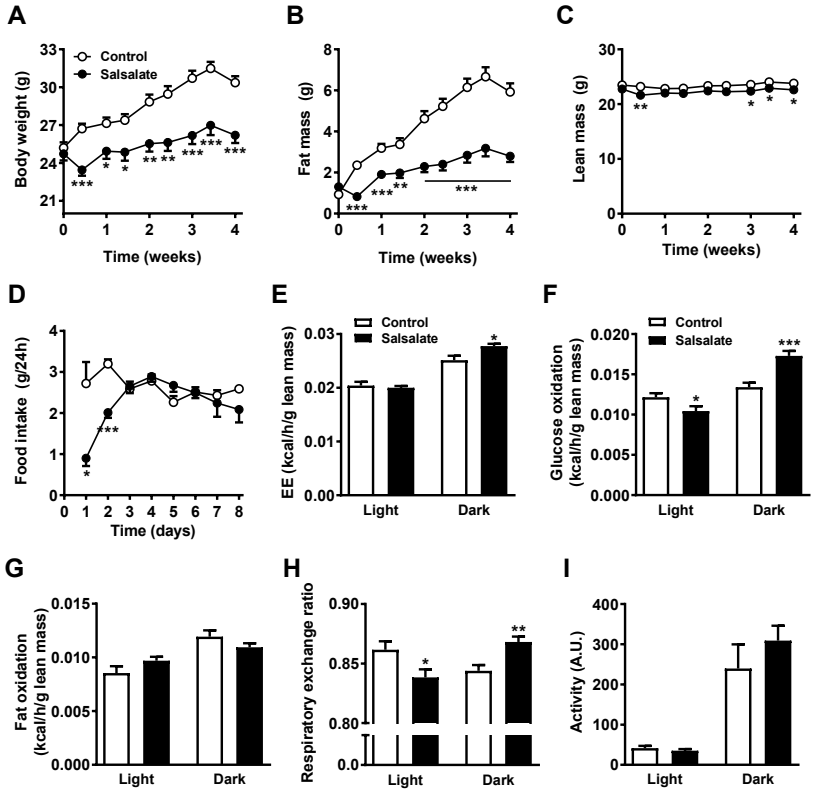

Supplementary figure 1. Salsalate prevents obesity and fat mass accumulation in wild type mice fed a high fat diet. *10-week old male wild type mice (C57Bl/6J background) were fed a high fat diet (HFD) without (open circles) or with (closed circles) salsalate for 4 weeks (A-D). Body weight (A), fat mass (B) and lean mass (C) were monitored throughout the experiment. Food intake was measured daily in the first week of the experiment (D). From day 5 to day 9 of salsalate treatment, mice were housed in fully automatic metabolic cages (LabMaster System; TSE Systems, Bad Homburg, Germany), which measured oxygen uptake (V_{O2}), carbon dioxide production (V_{CO2}) and caloric intake. Total energy expenditure (E) was calculated from V_{O2} and V_{CO2} using the Weir equation, and glucose oxidation (F) and fat oxidation (G) were calculated from V_{O2} and V_{CO2} as described previously (37). Respiratory exchange ratio (H) was also calculated from V_{O2} and V_{CO2}. Physical activity (I) was measured with infrared sensor frames. Measurements (E-H) were corrected for lean mass as determined by EchoMRI (EchoMRI-100, Houston, Texas, USA). EE = energy expenditure. Values represent means ± SEM (n=7-8). * p<0.05, ** p<0.01, *** p<0.001 vs control.*

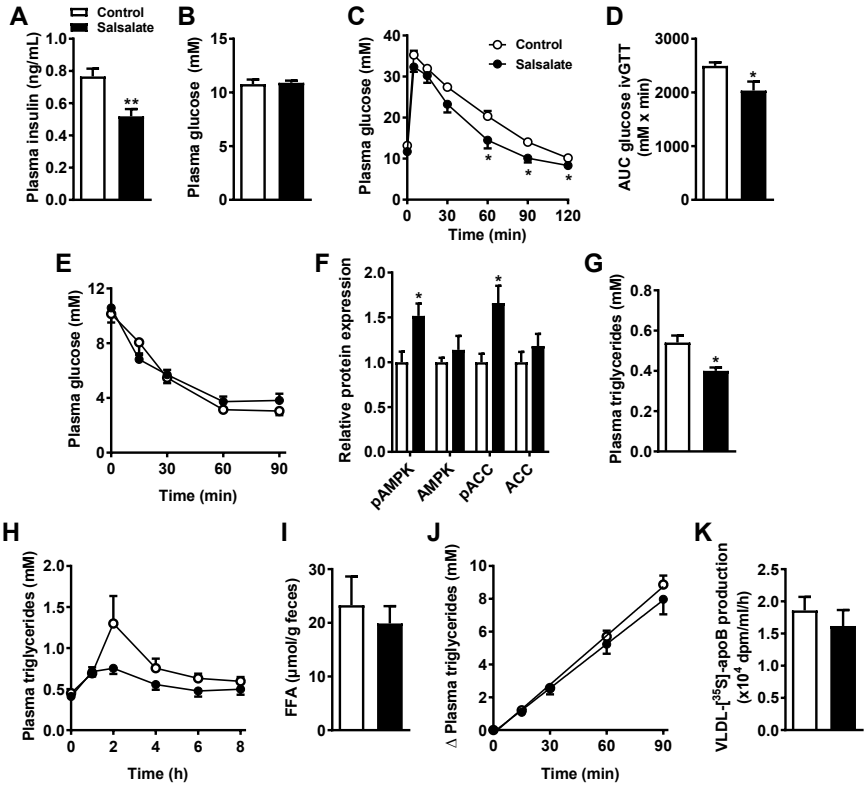

Supplementary figure 2. Salsalate improves glucose and triglyceride metabolism in wild type mice fed a high fat diet. *10-week old male wild type mice were fed a high fat diet (HFD) without (open circles/bars) or with (closed circles/bars) salsalate for 4 weeks. Blood samples from 6 h-fasted mice were collected by tail bleeding at different time points and plasma insulin (A), glucose (B) and triglyceride (G) levels were determined. After 4 weeks, 6 h fasted mice were i.v. injected with glucose and additional blood samples were taken at 5, 15, 30, 60, 90 and 120 min after injection (C-D). After 4 weeks, an insulin tolerance test was performed by injecting 6 h fasted mice i.p.with insulin (NovoRapid, Novo Nordisk, Denmark; 1 U/kg whole body mass) and measuring glucose at t = 15, 30, 60 and 90 min (E). Protein content in muscle was determined by Western blot (F). Postprandial triglyceride (TG) response was measured after 3 weeks of salsalate treatment. Animals were fasted for 6 h and a basal blood sample was drawn before an intragastric load of 200 µL olive oil (Carbonell, Traditional, Cordoba, Spain) was given. Blood samples were drawn 1, 2, 4, 6 and 8 h after the bolus via tail vein bleeding and plasma TG levels were measured (H). Feces was collected during the 3rd week of salsalate treatment. Feces was then weighed, freeze-dried and ground, and fecal fatty acids were determined by methyl esterification. To this end, 750 µL CH_3OH/NaOH (10 M)/H_2O (3:1:1 v/v) was added to the feces and samples were incubated and mixed in a thermomixer (600 rpm, 90°C) for 1 h. Then, 1050 µL of HCl (6 M)/hexane (3:7.7 v/v) was added before samples were vortexed and spun down 1 min at 14,000 rpm. The upper hexane layer was dried using N_2 and redissolved in 2% Triton X-100. Fatty acids were measured using the NEFA C kit (Wako Diagnostics, Instruchemie, Delfzijl) (I). After 4 weeks of salsalate treatment, hepatic VLDL production was determined. Mice were fasted for 4 h and anesthetized by intraperitoneal injection of 6.25 mg/kg acepromazine (Alfasan, Weesp), 6.25 mg/kg midazolam (Roche, Mijdrecht), and 0.31 mg/kg fentanyl (Janssen Pharmaceuticals, Tilburg). Mice were injected intravenously*

*with Tran[^{35}S] label (20 µCi/mouse; MP Biomedicals, Eindhoven) to label newly produced apolipoprotein B (apoB). After 30 min, at t = 0 min, Triton WR-1339 (Sigma-Aldrich) was injected intravenously (0.5 mg/g body weight, 10% solution in PBS) to block serum VLDL clearance. Blood samples were drawn before (t = 0) and at 15, 30, 60, and 90 min after injection of Triton and used for determination of plasma TG concentration (J). After 120 min, mice were exsanguinated via the retro-orbital plexus. VLDL was isolated from serum after density gradient ultracentrifugation at d < 1.006 g/ml by aspiration (38) and examined for incorporated ^{35}S-activity as a measure of ApoB production rate (K). AUC = area under the curve; FFA = free fatty acids. Values represent means ± SEM (n=5-8). * p<0.05, ** p<0.01 vs control.*

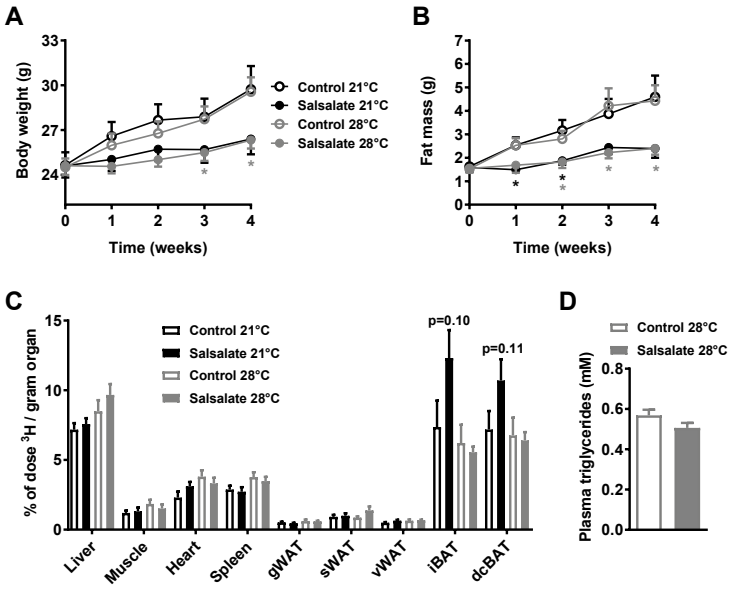

Supplementary figure 3. Effect of salsalate at thermoneutrality. *10-week old male wild type mice were housed at 21°C (black circles/bars) or 28°C (grey circles/bars) and fed a high fat diet (HFD) without (open circles/bars) or with (closed circles/bars) salsalate for 4 weeks. Body weight (A) and fat mass (B) were monitored throughout the experiment. A clearance experiment was performed in which 6 h-fasted mice were i.v. injected with [^{3}H]TO-labeled lipoprotein-like emulsion particles. After 15 min, mice were sacrificed and uptake of [^{3}H]TO-derived activity was determined in the organs (C). After 4 weeks of treatment, blood samples from 6 h-fasted mice were collected by tail bleeding and plasma triglyceride levels were determined (D). Values represent means ± SEM (n=7-8). * p<0.05 vs control. (g,s,v)WAT, gonadal, subcutaneous, visceral white adipose tissue; (i,dc)BAT, interscapular, dorsocervical brown adipose tissue.*

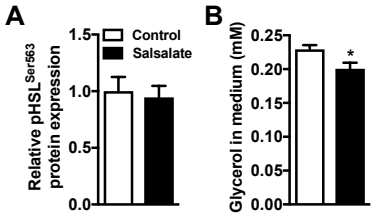

Supplementary figure 4. Effect of salsalate on 3T3-L1 cells. *3T3-L1 cells were cultured and differentiated into white adipocytes. White adipocytes were treated with 300 µM salsalate for 8 h. Protein content was determined by Western blot (A) and glycerol concentration in the culture medium was measured (B). Values represent means ± SD (n=3). * p<0.05 vs control.*

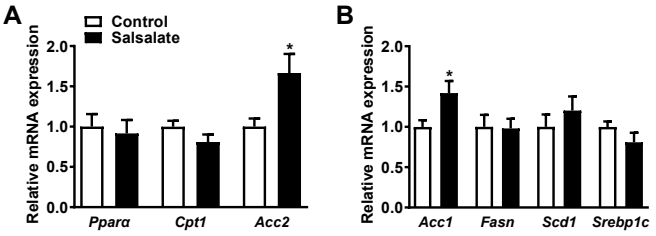

Supplementary figure 5. Effect of salsalate on genes involved in beta-oxidation and lipogenesis in gWAT of wild type mice fed a high fat diet. *10-week old male wild type mice were fed a high fat diet (HFD) without (open bars) or with (closed bars) salsalate for 4 weeks and gonadal white adipose tissue (gWAT) was collected. mRNA expression was determined by qRT-PCR (A-B). Values represent means ± SEM (n=7-8). * p<0.05 vs control.*

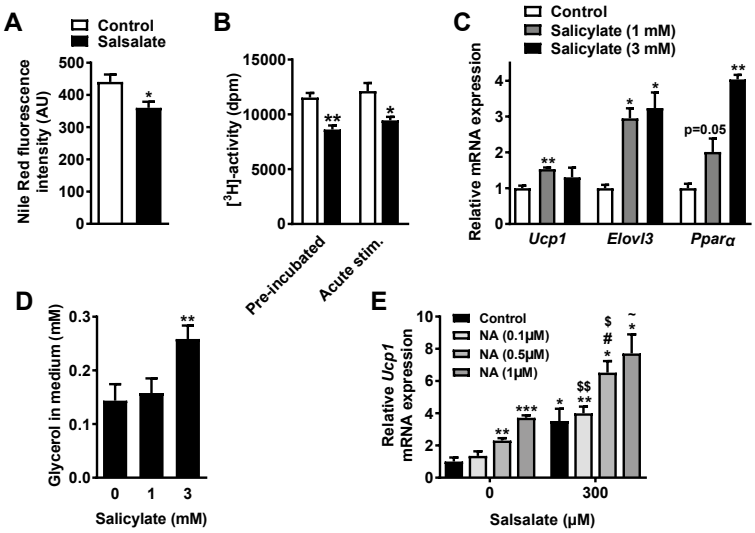

Supplementary figure 6. *In vitro* effects of salsalate and salicylate on T37i brown adipocytes. *T37i cells were cultured and differentiated into mature brown adipocytes. Cells (grown in 0.32 cm² wells) were treated with salsalate (300 μM) for 8 h, stained with 0.1 mg/mL Nile Red solution (Molecular probes, N-1142) for 2 h at 37°C and measured with a fluorimeter (Ex. 485 nm, Em. 590 nm). Values represent means ± SEM of 11 independent wells (A). To assess de novo lipogenesis, cells (grown in 3.8 cm² wells) were incubated at 37°C with HEPES buffer (29.8 g HEPES, 8.78 g NaCl, 4.66 g KCl, 1.12 g D-glucose, 18.8 g BSA, 0.132 g $CaCl_2$ in 1.125 L H_2O, pH 7.3), 100 nM insulin and [³H]glucose (~500,000 cpm). Cells were either pre-incubated with vehicle or salsalate for 6 h or the compound was added together with the [³H]glucose. After 2 h, cells were washed and 600 μL cold $CHCl_3/CH_3OH$ (1:1 v/v) was added. Cells were left on ice for 30 min, upon which the supernatant was isolated. Next, 125 μL H_2O was added and the samples were mixed and spun for 10 min at 3,500 rpm. The $CHCl_3$ layer was isolated and evaporated under N_2 and incorporation of [³H]glucose-derived radioactivity was quantified. Values represent means ± SEM of 4-5 independent wells (B). Cells were treated with salicylate (1 or 3 mM) for 8 h and mRNA expression was determined by qRT-PCR (C). In addition, glycerol concentration in the medium was assessed (D). Cells were treated with salsalate (300 μM) in the presence of increasing concentrations of noradrenalin (0.1 – 1 μM) for 8 h and Ucp1 mRNA expression was determined (E). NA = noradrenalin. Values represent means ± SD of 3-4 independent sets of RNA. * p<0.05, ** p<0.01 vs control , $ p<0.05, $$ p<0.01 vs NA, ~ p<0.10 vs NA and salsalate.*